HHS Public Access

Author manuscript

Anal Chim Acta. Author manuscript; available in PMC 2018 December 11.

Published in final edited form as:

Anal Chim Acta. 2018 December 11; 1037: 265–273. doi:10.1016/j.aca.2018.02.054.

Utilizing ion mobility spectrometry and mass spectrometry for the analysis of polycyclic aromatic hydrocarbons, polychlorinated biphenyls, polybrominated diphenyl ethers and their metabolites

Xueyun Zheng, **Kevin T. Dupuis**, **Noor A. Aly**, **Yuxuan Zhou**, **Francesca B. Smith**, **Keqi Tang**, **Richard D. Smith**, and **Erin S. Baker**[*]

Biological Sciences Division, Pacific Northwest National Laboratory, Richland, WA 99354, United States

Abstract

Polycyclic aromatic hydrocarbons (PAHs), polychlorinated biphenyls (PCBs) and polybrominated diphenyl ethers (PBDEs) are persistent environmental pollutants originating from incomplete combustion of organic materials and synthetic sources. PAHs, PCBs, and PBDEs have all been shown to have a significant effect on human health with correlations to cancer and other diseases. Therefore, measuring the presence of these xenobiotics in the environment and human body is imperative for assessing their health risks. To date, their analyses require both gas chromatography and liquid chromatography separations in conjunction with mass spectrometry measurements for detection of both the parent molecules and their hydroxylated metabolites, making their studies extremely time consuming. In this work, we characterized PAHs, PCBs, PBDEs and their hydroxylated metabolites using ion mobility spectrometry coupled with mass spectrometry (IMS-MS) and in combination with different ionization methods including electrospray ionization (ESI), atmospheric pressure chemical ionization (APCI) and atmospheric pressure photoionization (APPI). The collision cross section and m/z trend lines derived from the IMS-MS analyses displayed distinct trends for each molecule type. Additionally, the rapid isomeric and molecular separations possible with IMS-MS showed great promise for quickly distinguishing the parent and metabolized PAH, PCB, and PDBE molecules in complex environmental and biological samples.

GRAPHICAL ABSTRACT

[*]Corresponding author. 902 Battelle Blvd., P.O. Box 999, MSIN K8-98, Richland, WA 99352, United States. erin.baker@pnnl.gov (E.S. Baker).

Appendix A. Supplementary data

Supplementary data related to this article can be found at https://doi.org/10.1016/j.aca.2018.02.054.

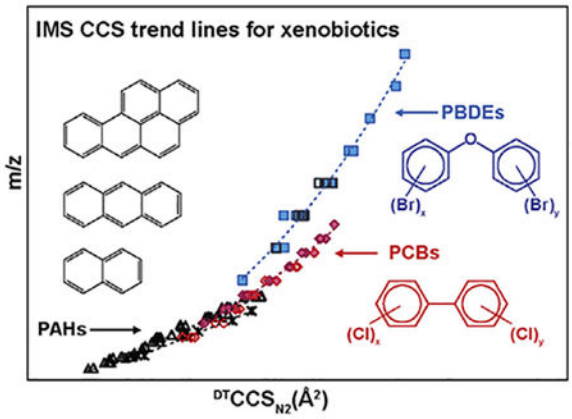

Keywords

Ion mobility spectrometry; Collision cross section; Xenobiotics; Polycyclic aromatic hydrocarbons; Polychlorinated biphenyls; Polybrominated diphenyl ethers; Electrospray ionization; Atmospheric pressure chemical ionization; Atmospheric pressure photoionization

1. Introduction

The characterization of xenobiotics in environmental and biological samples is extremely important for evaluating human exposure and subsequent health effects. Among them, polycyclic aromatic hydrocarbons (PAHs), polychlorinated biphenyls (PCBs) and polybrominated diphenyl ethers (PBDEs) are of great interest due to their persistence in the environment and known health effects. Specifically, PAHs are produced through incomplete combustion of organic materials from both natural and anthropogenic sources, such as forest fires, vehicle emissions, human wood burning, smoked meat, and industrial combustion of fossil fuels, which are some of the most widespread organic pollutants in the environment [1]. PAHs consist of fused benzene rings and are hydrophobic in nature with very low polarity. Representative structures for PAHs, such as naphthalene, anthracene and benzo(a) pyrene, are shown on Fig. 1a. Human can experience chronic exposure to PAHs present in the environment or their diets [2,3]. Furthermore, many PAHs have been identified as, or suspected to be, carcinogenic, mutagenic and teratogenic. Thus, evaluating the presence of these xenobiotic classes in the environment and human body is essential for assessing and understanding their health risks [4].

PCBs are synthetic organochlorine chemicals used in many past industrial products, including electrical capacitors, transformers, paints, lubricants, adhesives and ceiling and floor tiles [5]. Ultimately the production of PCBs was terminated due to the recognition of their accumulation in both the environment and living organisms and resistance to degradation [6,7]. PCBs consist of two six-carbon rings linked by a single carbon-carbon bond (biphenyl) with chlorine atoms substituted for hydrogen atoms at any of the 10 possible positions. The general structure for PCBs and their nomenclature are shown in Fig. 1a. PCBs are lipid-soluble due to the nonpolar properties and therefore can be taken up through inhalation, dermal contact or food intake. Exposure to PCBs has been shown to

suppress human immune systems and increase the risk of diseases such as infection, cancer and infertility [8–11]. PCB exposure is also of great concern for pregnant women as it has been linked to infants with low birth weights, and exposure during fetal and early life can have significant effects on IQ and behavior [5,12].

The third class of xenobiotics analyzed in this study was the PBDEs. PBDEs are widely used as a flame-retardant and have been found in consumer goods, such as electrical equipment, paints, textiles and construction materials [13]. PBDEs are dicyclic aromatic ethers with bromine atoms substituted for the hydrogen atoms in any of the 10 possible positions (Fig. 1a). Similar in structure to PCBs, PBDEs resist degradation and are also persistent pollutants in the environment. Human exposure to PBDEs have increased health risk, including tumors, neurodevelopmental toxicity and thyroid hormone imbalance [14,15]. Thus, the combined risks associated with PAHs, PCBs and PBDEs makes their thorough characterization and rapid analyses of great interest to both the public and scientific community.

While the intact PAHs, PCBs and PBDEs in environmental samples can be analyzed directly by MS based techniques, their analysis in human body fluids is complicated by their metabolism to hydroxylated forms; i.e. OH-PAHs, OH-PCBs and OH-PBDEs. Therefore, it is desirable to measure both the intact xenobiotics and their metabolites to fully assess exposure and human health risk. Due to their nonpolar properties, however, these molecules are generally missed by conventional MS-based metabolomics approaches. Gas chromatography-mass spectrometry (GC-MS) has been one of the most widely used methods for their analyses, but it is slow and requires additional chemical derivatization approaches which can cause degradation [4,12,16]. In most analyses, the hydroxylated metabolites are analyzed separately by liquid chromatography-mass spectrometry (LC-MS) [17,18], making multiple measurements necessary for each sample. Long LC separation times are also required due to their high structural similarity and numerous isomers. Thus, new broadly useful and higher throughput approaches are desired for effective analyses of intact PAHs, PCBs, PDBEs and their metabolites. Ion mobility spectrometry coupled with mass spectrometry (IMS-MS) is an attractive approach for these studies due to its capabilities of separating isomeric structures on a millisecond time scale and enabling rapid structural and mass analyses [19–22] (Schematic for IMS separation principle is shown in Fig. 1b). Previous IMS analyses of a small number of PAH and PBDE standards illustrated that IMS is capable of analyzing and separating these nonpolar molecules [23–26]. In this work we further evaluated IMS-MS for the rapid characterization of PAHs, PCBs, PBDEs and their hydroxylated metabolites with different ionization methods including electrospray ionization (ESI), atmospheric pressure chemical ionization (APCI) and atmospheric pressure photoionization (APPI).

2. Materials and methods

2.1. Chemicals, solvents and sample preparations

PAH, PCB and PBDE standards were purchased from Sigma-Aldrich (St. Louis, MO) and AccuStandard Inc. (New Haven, CT) and high purity solvents including water, methanol, acetonitrile, hexane, acetone, toluene and dichloromethane were purchased from Thermo Fisher Scientific (Waltham, MA). The PAH, PCB and PBDE standards were dissolved in

toluene and diluted in v/v 50:50 methanol:acetone or acetonitrile to a final concentration of 1–5 μM.

2.2. Drift tube IMS analysis and CCS measurements

An Agilent 6560 IMS-QTOF MS (Agilent Technologies, Santa Clara) equipped with the gas kit upgrade was utilized for all of the drift tube IMS (DTIMS) measurements in this work [27,28]. PAHs, PCBs and PBDEs were ionized using APCI and/or APPI where radical, protonated and deprotonated forms were observed. Hydroxylaed PAHs, PCBs and PBDEs were ionized using ESI, APCI and/or APPI. For the DTIMS CCS measurements, ions were passed through the inlet glass capillary, focused by a high pressure ion funnel, and accumulated in an ion funnel trap. Ions were then pulsed into the78.24 cm long IMS drift tube filled with ~3.95 torr of nitrogen gas, where they travelled under the influence of a weak electric field (10–20 V/cm). Ions exiting the drift tube were refocused by a rear ion funnel prior to QTOF MS detection and their arrival time (t_A) was recorded. The reduced mobility (K_0, the mobility scaled for standard temperature and pressure) was then determined from the instrument parameters by plotting t_A versus p/V [29]:

$$t_A = \frac{L^2}{K_0}\left(\frac{273.15}{760T}\right)\left(\frac{p}{V}\right) + t_0$$

where L is the drift length, V is the drift voltage, t_0 is the time ion spending outside of the drift cell, T is the drift gas temperature, and p is the drift gas pressure. CCS values (Ω) were then calculated using the reduced mobility and kinetic theory [29]:

$$\Omega = \frac{3q}{16N}\left(\frac{2\pi}{\mu k_B T}\right)^{1/2}\frac{1}{K_0}$$

where q is the ion charge, N is the buffer gas number density at STP, m is the reduced mass of the ion nitrogen collision pair, and k_B is the Boltzmann constant. All the CCS values were measured using seven stepped electric field voltages to obtain the most accurate slope for calculation of K_o and each sample was analyzed in both positive and negative ionization modes. CCS values are listed in Table S1. The detailed instrumental settings are given in the Supplemental Methods, Tables S2–S4, and follow those previously published in an interlaboratory examination [30] and a drift tube IMS CCS database study [31]. Each sample was measured in triplicate and relative standard deviations (RSDs) were measured for all analytes. The Agilent IM-MS Browser software was utilized for all stepped field CCS calculations.

3. Results and discussion

In this study, we utilized IMS-MS to characterize over 120 standards corresponding to PAH, PCB, and PBDE compounds and their metabolites. Isomers for each xenobiotic class were examined with IMS to understand if separation was achievable. The IMS collision cross sections (CCS) and m/z trends were also studied for the whole collection of molecules, allowing in depth structural information on each class. As a first step of the analyses, we

evaluated different ionization methods including ESI, APCI and APPI to determine the best ionization method for each compound type. All raw data files are available on the NIH Metabolomics Workbench (DataTrack: 1322), if further evaluation is desired.

3.1. Different ionization techniques for polar and nonpolar molecules

ESI is one of the most commonly used ionization techniques for liquid samples and is the preferred method for small polar molecules, including amino acids, fatty acids, organic acids, glycans and peptides due to its soft nature. ESI also creates multiply charged ions, enabling the analysis of very large molecules. However, compounds with lower polarity such as most pesticides, herbicides, antibiotics, PAHs, PCBs, PBDEs and their metabolites do not ionize well with ESI. Other low energy ionization methods such as APCI and APPI are often used to effectively ionize these chemicals while keeping them intact. As shown in Fig. 2, in APCI, analytes in solution are first converted into gas phase molecules by a high temperature vaporizer and subsequently ionized directly with a corona discharge at atmospheric pressure. The ionization of APPI is initiated by 10 eV photons emitted from a UV lamp, which ionize compounds with ionization energies lower than this value. Most organic compounds can be ionized while background gases and the typical solvents are left out. Due to these characteristics, APPI is more selective than APCI, which also ionizes atmospheric gases and solvents with the corona discharge-initiated ionization reactions [32]. Moreover, a dopant such as acetone or toluene is often used in APPI, which can be ionized efficiently and acts as a charge carrier, leading to better sensitivity than APCI in many cases [32–34].

In this work, we specifically explored the capabilities of ESI, APPI and APCI for the analysis of PAHs, PCBs, and PBDEs and their hydroxylated metabolites. We found, as expected, that PAHs, PCBs and PBDEs were ionized efficiently by either APCI or APPI, but not ESI. However, their hydroxylated metabolites, OH-PAHs, OH-PCBs and OH-PBDEs, were ionized effectively by all three techniques. PAHs were observed to form both protonated and radical ions in the positive ionization mode during APCI and APPI, which is consistent with previous studies [35,36]. APCI was also found to generate a higher fraction of protonated species, while APPI mainly produced radical species and much less of the protonated versions. For example, the two PAH isomers, 3,6-dimethylphenanthrene (36T) and 2,3-dimethylanthracene (23D), illustrated vastly different ionization properties with the APCI and APPI processes (Fig. 3). In APCI, both 36T and 23D displayed a large fraction of protonated species, especially 23D which had a dominant protonated form. However in APPI, both 36T and 23D primarily formed the radical species. As a result the mass spectra obtained from APPI was much simpler to interpret for both identification and quantification than those obtained from APCI. Due to similar results for other molecules, APPI was selected as our preferred ionization method for the analysis of PAH, PCB and PDBE compounds in this study.

3.2. IMS separation of PAHs and OH-PAHs

Since both radical and protonated species are possible with APPI and APCI, we were also interested in understanding their CCS size differences. In Fig. 4A, the different ionization forms of benzo(a) pyrene (BAP) and benzo(k)fluoranthene (BKF) were evaluated. BAP and

BKF are isomers with subtle differences in the ring arrangement. Therefore, we observed that both the radical and protonated forms of each could be partially separated with IMS with BKF having a longer arrival time and larger structure than BAP in both ionization forms. Interestingly, the protonated arrival times and CCS values were larger for both molecules than that of the radical forms, indicating the extra proton has an effect on the overall size of the molecule.

The hydroxylated metabolites of PAHs (OH-PAHs) can be ionized by either ESI, APCI or APPI due to their slightly increased polarity from the hydroxyl group addition. In these studies, the OH-PAHs were only observed in the negative ion mode as deprotonated ions. For example, the IMS profiles of the deprotonated isomers, 2,3-dihydroxylnaphthanlene (23A), 1,5-dihydroxylnaphanlene (1DH) and 2,6-dihydroxylnaphanlene (26T) are shown in the left panel of Fig. 4B, where 23A has the shortest arrival time, while 26T has the longest. Since 23A has two hydroxyl groups on adjacent carbons, it therefore has a more compact conformation. The two hydroxyl groups for 1DH and 26T have more distance on the phenyl rings and therefore result in more extended structures, especially for 26T, where the hydroxyl groups have the greatest separation. However, as the size of the PAH molecule increases, the position of the hydroxyl group does not have as significant of an effect on the size of the OH-PAH molecules. For example, benzo(a)pyrene with a hydroxyl group at either the 7 carbon position (7-hydroxybenzo(a) pyrene, 7AR) or 12 carbon position (12-hydroxybenzo(a)pyrene, 1AE) has a very similar arrival time and cannot be separated by IMS (Fig. 4B right panel). Thus, higher resolution IMS separations or a combination of other separation techniques (i.e. GC or LC) are needed to distinguish these subtle structural differences.

3.3. Isomer separation of PCBs and PBDEs

In order to evaluate the capability of IMS to separate other xenobiotics compounds, PCBs and PBDEs were investigated. Examples of IMS separations for PCB and OH-PCB isomers were shown in Fig. 5. PCBs can by ionized efficiently with APCI and APPI, but not ESI due to their low polarities. In our analyses, the PCB molecules were observed to lose one chlorine and add an oxygen resulting in the negatively charged ($[M\text{-}Cl + O]^-$) species in both APCI and APPI. While many of the PCB isomeric structures were very similar, we were still able to distinguish most of them with IMS. For example, 2,2′,4,5′,6-Pentachlorobiphenyl (PCB-103) and 3,3′,4,4′,5-Pentachlorobiphenyl (PCB-126), which are two PCB isomers with five chlorines on the biphenyl rings, can be almost baseline separated by IMS. PCB-126 which has two chlorines on the para carbons has a more extended structure than PCB-103, which only has a single chlorine on the para carbon and the others distributed on the ortho or meta positions that are less extended. In addition, it has been suggested that PCBs with no chlorine in the ortho positions exist primarily in a planar structure, and when two or more chlorines exist in the ortho positions, the molecules are likely to form a three-dimensional structure [5]. Therefore PCB-103 with three chlorines at the ortho positions (2,2′,6′) is more likely to adapt a more compact three-dimensional structure, while PCB-126 with no chlorines in the ortho positions forms a more extended planar structure and has a larger size than PCB-103.

The hydroxylated PCBs (OH-PCBs) were also characterized with ESI, APCI and APPI and detected as deprotonated $[M\ H]^-$ species. Since both the parent ions and metabolite species were detected in similar forms with APCI and APPI due to the addition of oxygen for the parent molecules, ESI was necessary to evaluate the presence of hydroxylated metabolites since the parent ions are not present in these analyses. When the OH-PCB metabolites were analyzed with IMS, separation was again possible. For example, 2-Hydroxy-2′,3′,4′,5,5′-pentachlorobiphenyl (6′-OH-PCB-106) and 4-Hydroxy-2′,3,3′,4′,5′-pentachlorobiphenyl (4′-OH-PCB-106), two monohydroxylated metabolite isomers of 5-chlorine PCB-106 were separated by IMS with 4′-OH-PCB-106 having a larger size than 6′-OH-PCB-106 due to its hydroxyl group being present at the *para* carbon with the largest distance from each other. This is also consistent with 6′-OH-PCB-106 having two groups (chlorine and hydroxyl groups) at the ortho carbons forming a more compact three-dimensional configuration, while 4′-OH-PCH-106 remains as a planar structure.

Similar to the PCBs, the PBDE parent molecules were observed in their $[M\text{-}Br + O]^-$ form with both APCI and APCI, and could not be ionized by ESI. Again separation of the isomers was possible as illustrated in Fig. 6 for 2,3,4,5,6-Pentabromodiphenyl ether (PBDE-116) and 2,2′,3,4,4′-Pentabromodiphenyl ether (PBDE-85), which had very different IMS profiles allowing baseline separation. This is expected as all of the bromines for PBDE-116 are localized on one phenyl ring, while the bromines for PBDE-85 are distributed on each phenyl ring, resulting in a larger size. The hydroxylated PBDEs (OH-PBDEs) were also evaluated and detected as deprotonated ions in ESI, APPI and APCI. Again since both the parent PBDE ions and metabolite species were detected in similar forms with APCI and APPI due to the addition of oxygen, ESI analyses were necessary to evaluate the presence of the hydroxylated metabolites. The OHPBDE were also analyzed with IMS and again separation was possible as shown by the 5-bromine PBDEs, 3-OH-PBDE-100 and 4′-OH-PBDE-101, where 3-OH-PBDE-100 had a smaller structure than 4′-OH-PBDE-101 due to its bromine placements. Thus, the isomeric separations of the PCBs, PBDEs, and their metabolites show great promise for using the rapid IMS analyses on these xenobiotic compounds in more complex mixtures.

3.4. IMS-MS trend lines for PAHs, PCBs and PBDEs

To understand the structural differences of PAHs, PCBs, PBDEs and their metabolites, over 120 standards were characterized by IMS-MS. The measured CCS and corresponding m/z values are shown in Fig. 7. The trend lines for the PAHs clearly illustrated that both the protonated parents, radical cations, and deprotonated hydroxylated metabolites are crowded in the lower left region of the CCS vs m/z plot. This suggests PAHs are smaller in mass (100–350 Da) and structure than PCBs or PBDEs since they do not have chlorine or bromine functional groups. Both PCBs and PBDEs gradually grew in CCS as the number of the chlorines or bromines increased. Moreover, the CCS values for PCBs are larger than that of the PBDEs with the same m/z values, indicating PCB have a larger structure than PBDE. While this seems counterintuitive when just comparing the presence of chlorine or bromine, the ring attachment must also be considered. Since the phenyl groups for the PCBs are connected through a carbon-carbon bond, the two aromatic rings can rotate freely. On the other hand, the two phenyl rings in PBDEs are connected through an oxygen atom forming

an ether linkage. The electron density of the phenyl rings and the oxygen are conjugated to form a stable planar structure and the phenyl rings have a more compact backbone, causing the PBDEs to have a smaller size than the PCBs. The CCS information obtained for the PAHs, PCBs, and PBDEs provide the basis for future analyses of complex environmental and biological samples for the identification of both known and unknown molecules.

4. Conclusions

In this work, we characterized over 120 PAHs, PCBs, PBDEs and their metabolites using IMS-MS with APPI, APCI and ESI sources. The PAHs were observed as both protonated and radical ions, while the OH-PAHs were detected as deprotonated species. PCBs and PBDEs were observed as $[M\text{-}Cl + O]^-$ and $[M\text{-}Br\ O]^-$ and their OH PCB and OH-PBDE metabolites were detected as deprotonated ions. Since both the parent ions and metabolite species for the PCBs and PBDEs were detected in similar forms with APCI and APPI, ESI analyses are necessary to determine when hydroxylated metabolites are present in complex samples. In the analysis of the isomers for the PAHs, PCBs, PDBEs, and their metabolites, many were distinguished by IMS with some almost baseline separated. The ability to distinguish the isomers of each xenobiotic class illustrates the great promise of IMS for analyzing and separating these compounds in future studies of complex environmental and biological samples. While many IMS isomeric separations were illustrated in this manuscript for PAHs, PCBs, PBDEs and their metabolites, some if the isomers had very close CCS values as shown in Table S1. This occurs due to the rigid nature of PAHs, PCBs and PBDEs and indicates that either additional separations (i.e. LC or GC) or higher resolution IMS techniques, such as those recently developed using structures for lossless ion manipulations (SLIM) [37–39], may be required. However, this study lays the ground work for determining which ionization sources are needed and what species will be detected for the PAH, PCB, and PBDE molecules of interest.

Supplementary Material

Refer to Web version on PubMed Central for supplementary material.

Acknowledgements

The authors would like to acknowledge Drs. Keri Hornbuckle and Rachel Marek from the University of Iowa for insightful discussions on PAH and PCB extractions and analyses. The authors would also like to thank Dr. Kim Anderson from Oregon State University and Dr. Ivan Rusyn from Texas A&M University for some of the PAH standards. Portions of this research were supported by grants from the National Institute of Environmental Health Sciences of the NIH (R01 ES022190), National Institute of General Medical Sciences (P41 GM103493), NIH (P42 ES027704), and the Laboratory Directed Research and Development Program at Pacific Northwest National Laboratory. This research utilized capabilities developed by the Pan-omics program (funded by the U.S. Department of Energy Office of Biological and Environmental Research Genome Sciences Program). This work was performed in the W. R. Wiley Environmental Molecular Sciences Laboratory (EMSL), a DOE national scientific user facility at the Pacific Northwest National Laboratory (PNNL). PNNL is operated by Battelle for the DOE under contract DE-AC05–76RL0 1830.

References

[1]. Abdel-Shafy HI, Mansour MSM, A review on polycyclic aromatic hydro-carbons: source, environmental impact, effect on human health and remediation, Egypt. J. Petrol 25 (1) (2016) 107–123.

[2]. Kim K-H, et al., A review of airborne polycyclic aromatic hydrocarbons (PAHs) and their human health effects, Environ. Int 60 (Supplement C) (2013) 71–80. [PubMed: 24013021]

[3]. Domingo JL, Nadal M, Human dietary exposure to polycyclic aromatic hydrocarbons: a review of the scientific literature, Food Chem. Toxicol 86 (Supplement C) (2015) 144–153. [PubMed: 26456806]

[4]. Pleil JD, et al., Cumulative exposure assessment for trace-level polycyclic aromatic hydrocarbons (PAHs) using human blood and plasma analysis,J. Chromatogr. B 878 (21) (2010) 1753–1760.

[5]. Carpenter David O, Polychlorinated biphenyls (PCBs): routes of exposure and effects on human health, Rev. Environ. Health 21 (1) (2006) 1–23. [PubMed: 16700427]

[6]. Ulbrich B, Stahlmann R, Developmental toxicity of polychlorinated biphenyls (PCBs): a systematic review of experimental data, Arch. Toxicol 78 (5) (2004) 252–268. [PubMed: 15064922]

[7]. Breivik K, et al., Towards a global historical emission inventory for selected PCB congeners d a mass balance approach: 3, An update Sci. Total Environ 377 (2) (2007) 296–307. [PubMed: 17395248]

[8]. Meeker JD, Hauser R, Exposure to polychlorinated biphenyls (PCBs) and male reproduction, Syst. Biol. Reprod. Med 56 (2) (2010) 122–131. [PubMed: 20377311]

[9]. Helmfrid I, et al., Health effects and exposure to polychlorinated biphenyls (PCBs) and metals in a contaminated community, Environ. Int 44 (Supplement C) (2012) 53–58. [PubMed: 22336529]

[10]. Ali I, et al., Exposure to polychlorinated biphenyls and prostate cancer: population-based prospective cohort and experimental studies, Carcinogen-esis 37 (12) (2016) 1144–1151.

[11]. Donat-Vargas C, et al., Dietary exposure to polychlorinated biphenyls and risk of breast, endometrial and ovarian cancer in a prospective cohort, Br. J. Canc 115 (9) (2016) 1113–1121.

[12]. Marek RF, et al., PCBs and OH-PCBs in serum from children and mothers in urban and rural U.S. Communities, Environ. Sci. Technol 47 (7) (2013) 3353–3361. [PubMed: 23452180]

[13]. Frederiksen M, et al., Human internal and external exposure to PBDEs e a review of levels and sources, Int. J. Hyg Environ. Health 212 (2) (2009) 109–134. [PubMed: 18554980]

[14]. Siddiqi MA, Laessig RH, Reed KD, Polybrominated diphenyl ethers (PBDEs): new pollutants-old diseases, Clin. Med. Res 1 (4) (2003) 281–290. [PubMed: 15931321]

[15]. Herbstman JB, et al., Prenatal exposure to PBDEs and neurodevelopment, Environ. Health Perspect 118 (5) (2010) 712–719. [PubMed: 20056561]

[16]. Awad AM, et al., Occurrence and distribution of two hydroxylated polychlorinated biphenyl congeners in chicago air, Environ. Sci. Technol. Lett 3 (2) (2016) 47–51. [PubMed: 30246046]

[17]. Fan R, et al., Fast and simultaneous determination of urinary 8-Hydroxy-20-deoxyguanosine and ten monohydroxylated polycyclic aromatic hydrocarbons by liquid chromatography/tandem mass spectrometry, Chem. Res. Toxicol 25 (2) (2012) 491–499. [PubMed: 22250670]

[18]. Lung S-CC, Liu C-H, Fast analysis of 29 polycyclic aromatic hydrocarbons (PAHs) and nitro-PAHs with ultra-high performance liquid chromatography-atmospheric pressure photoionization-tandem mass spectrometry, Sci. Rep 5 (2015) 12992. [PubMed: 26265155]

[19]. Baker ES, et al., Enhancing bottom-up and top-down proteomic measurements with ion mobility separations, Proteomics 15 (16) (2015) 2766–2776. [PubMed: 26046661]

[20]. Kyle JE, et al., Uncovering biologically significant lipid isomers with liquid chromatography, ion mobility spectrometry and mass spectrometry, Analyst 141 (5) (2016) 1649–1659. [PubMed: 26734689]

[21]. Burnum-Johnson KE, Baker ES, Metz TO, Characterizing the lipid and metabolite changes associated with placental function and pregnancy complications using ion mobility spectrometry-mass spectrometry and mass spectrometry imaging, Placenta 60 (Suppl. 1) (2017 12) S67–S72. [PubMed: 28392013]

[22]. May JC, Gant-Branum RL, McLean JA, Targeting the untargeted in molecular phenomics with structurally-selective ion mobility-mass spectrometry, Curr. Opin. Biotechnol 39 (39) (2016) 192–197. [PubMed: 27132126]

[23]. Baim MA, Eatherton RL, Hill HH, Ion mobility detector for gas chromatography with a direct photoionization source, Anal. Chem 55 (11) (1983) 1761–1766.

[24]. Castellanos A, et al., Fast screening of polycyclic aromatic hydrocarbons using trapped ion mobility spectrometry - mass spectrometry, Anal. Meth 6 (23) (2014) 9328–9332.

[25]. Benigni P, Marin R, Fernandez-Lima F, Towards unsupervised polyaromatic hydrocarbons structural assignment from SA-TIMS eFTMS data, Int. J. Ion Mobil. Spectrom 18 (3) (2015) 151–157. [PubMed: 26525904]

[26]. Adams KJ, et al., Isomer separation of polybrominated diphenyl ether metabolites using nanoESI-TIMS-MS, Int. J. Ion Mobil. Spectrom 19 (2) (2016) 69–76. [PubMed: 27642261]

[27]. May JC, et al., Conformational ordering of biomolecules in the gas phase: nitrogen collision cross sections measured on a prototype high resolution drift tube ion mobility-mass spectrometer, Anal. Chem 86 (4) (2014) 2107–2116. [PubMed: 24446877]

[28]. Ibrahim YM, et al., Development of a new ion mobility time-of-flight mass spectrometer, Int. J. Mass Spectrom 377 (2015) 655–662. [PubMed: 26185483]

[29]. Mason EA, McDaniel EW, Kinetic theory of mobility and diffusion: sections5.1 – 5.2, in: Transport Properties of Ions in Gases, Wiley-VCH Verlag GmbH & Co. KGaA, 2005, pp. 137–193.

[30]. Stow SM, et al., An interlaboratory evaluation of drift tube ion mobility - mass spectrometry collision cross section measurements, Anal. Chem 89 (17) (2017) 9048–9055. [PubMed: 28763190]

[31]. Zheng X, et al., A structural examination and collision cross section database for over 500 metabolites and xenobiotics using drift tube ion mobility spec-trometry, Chem. Sci 8 (11) (2017) 7724–7736. [PubMed: 29568436]

[32]. Kauppila TJ, Syage JA, Benter T, Recent developments in atmospheric pressure photoionization-mass spectrometry, Mass Spectrom. Rev 9999 (2015) 1–27.

[33]. Hanold KA, et al., Atmospheric Pressure Photoionization. 1. General Properties for LC/MS, Anal. Chem 76 (10) (2004) 2842–2851. [PubMed: 15144196]

[34]. Kauppila TJ, et al., Negative ion-atmospheric pressure photoionization-mass spectrometry, J. Am. Soc. Mass Spectrom 15 (2) (2004) 203–211. [PubMed: 14766288]

[35]. Ghislain T, Faure P, Michels R, Detection and monitoring of PAH and oxy-PAHs by high resolution mass spectrometry: comparison of ESI, APCI and APPI source detection, J. Am. Soc. Mass Spectrom 23 (3) (2012) 530–536. [PubMed: 22281813]

[36]. Vaikkinen A, Kauppila TJ, Kostiainen R, Charge exchange reaction in dopant-assisted atmospheric pressure chemical ionization and atmospheric pressure photoionization, J. Am. Soc. Mass Spectrom 27 (8) (2016) 1291–1300. [PubMed: 27126470]

[37]. Zheng X, et al., Distinguishing d- and l-aspartic and isoaspartic acids in amyloid [small beta] peptides with ultrahigh resolution ion mobility spectrometry, Chem. Commun 53 (56) (2017) 7913–7916.

[38]. Zheng X, et al., Structural elucidation of cis/trans dicaffeoylquinic acid photoisomerization using ion mobility spectrometry-mass spectrometry, J. Phys. Chem. Lett 8 (2017) 1381–1388. [PubMed: 28267339]

[39]. Wojcik R, et al., Lipid and glycolipid isomer analyses using ultra-high resolution ion mobility spectrometry separations, Int. J. Mol. Sci 18 (1) (2017) 183.

HIGHLIGHTS

- Cross sections for >120 PAHs, PCBs, PBDEs and their metabolites were characterized using IMS-MS with APPI, APCI and ESI.
- Many of the isomers for the PAHs, PCBs, PDBEs, and their metabolites, were distinguished by IMS.
- Structural trend lines were observed for the xenobiotic classes with PAHs having the smallest sizes relative to m/z.

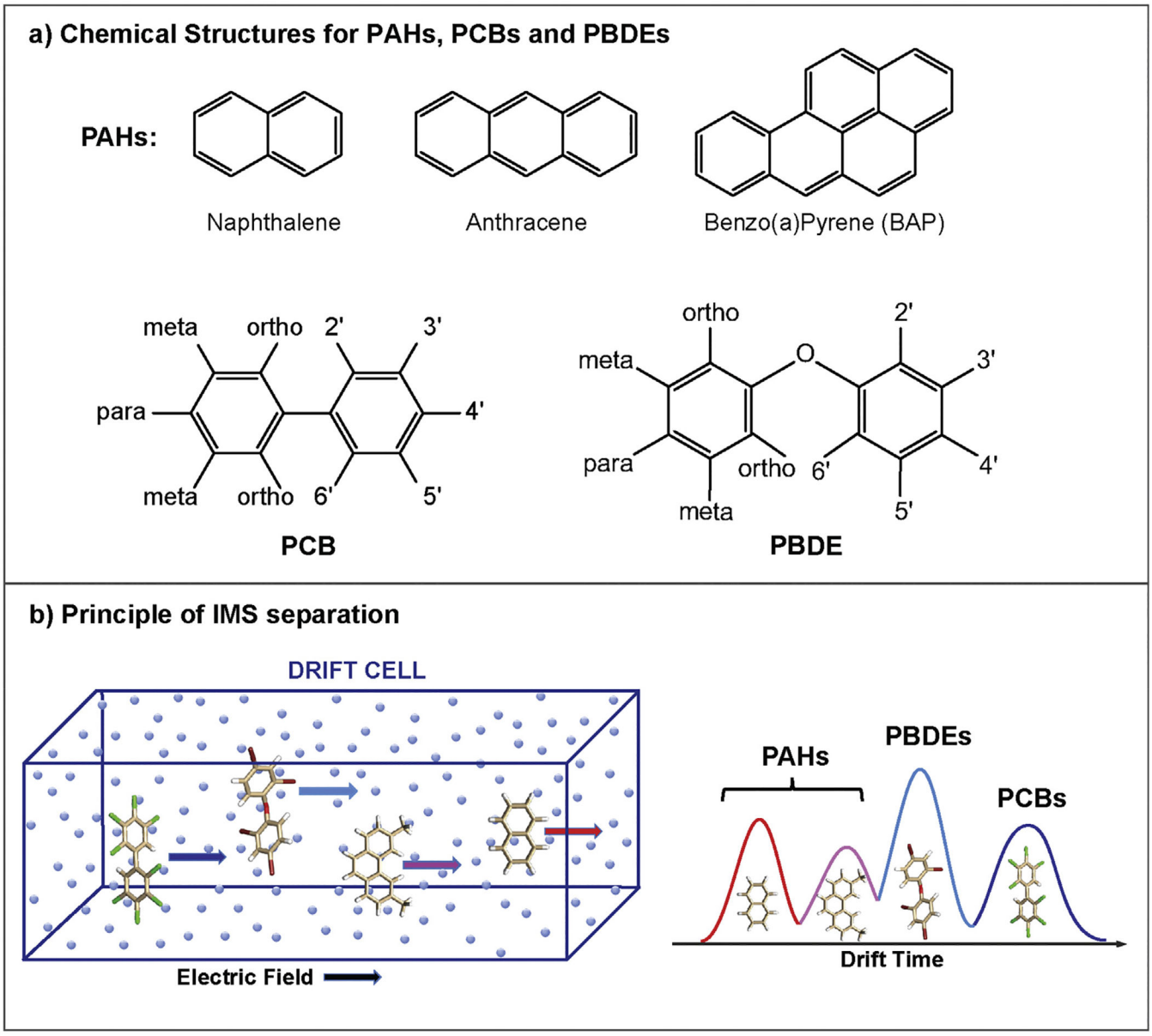

Fig. 1.

a) Representative chemical structures of PAHs, PCBs and PDBEs. PAHs consist of fused benzene rings (i.e. naphthalene, anthracene and benzo(a)pyrene) as shown in the top panel, while the different phenyl linkages and nomenclature of PCBs and PBDEs are shown below. For the PCBs and PDBEs, chlorines and bromines are substituted for hydrogens at the 10 possible positions on the two phenyl rings and they are numbered as 2 to 6 on the first ring and 2′ to 6′ on the second. The 2, 2′, 6 and 6′ positions closest to the diphenyl (or diphenyl ether) bond are described as ortho, while para corresponds to the 4 and 4′ positions and meta has the 3, 3′, 5 and 5′ positions. The number and location of chlorines and bromines determine both the physical and biological activities of each molecule. b) A schematic of ion mobility spectrometry separation principle. Briefly, in an IMS separation, the ions travel through a drift cell filled with buffer gas (i.e. N_2) under the influence of a

weak electric field. The separation depends on the mass, charge and the shape of the ions. For isomers with the same m/z, compact structures will travel faster than more extended structures.

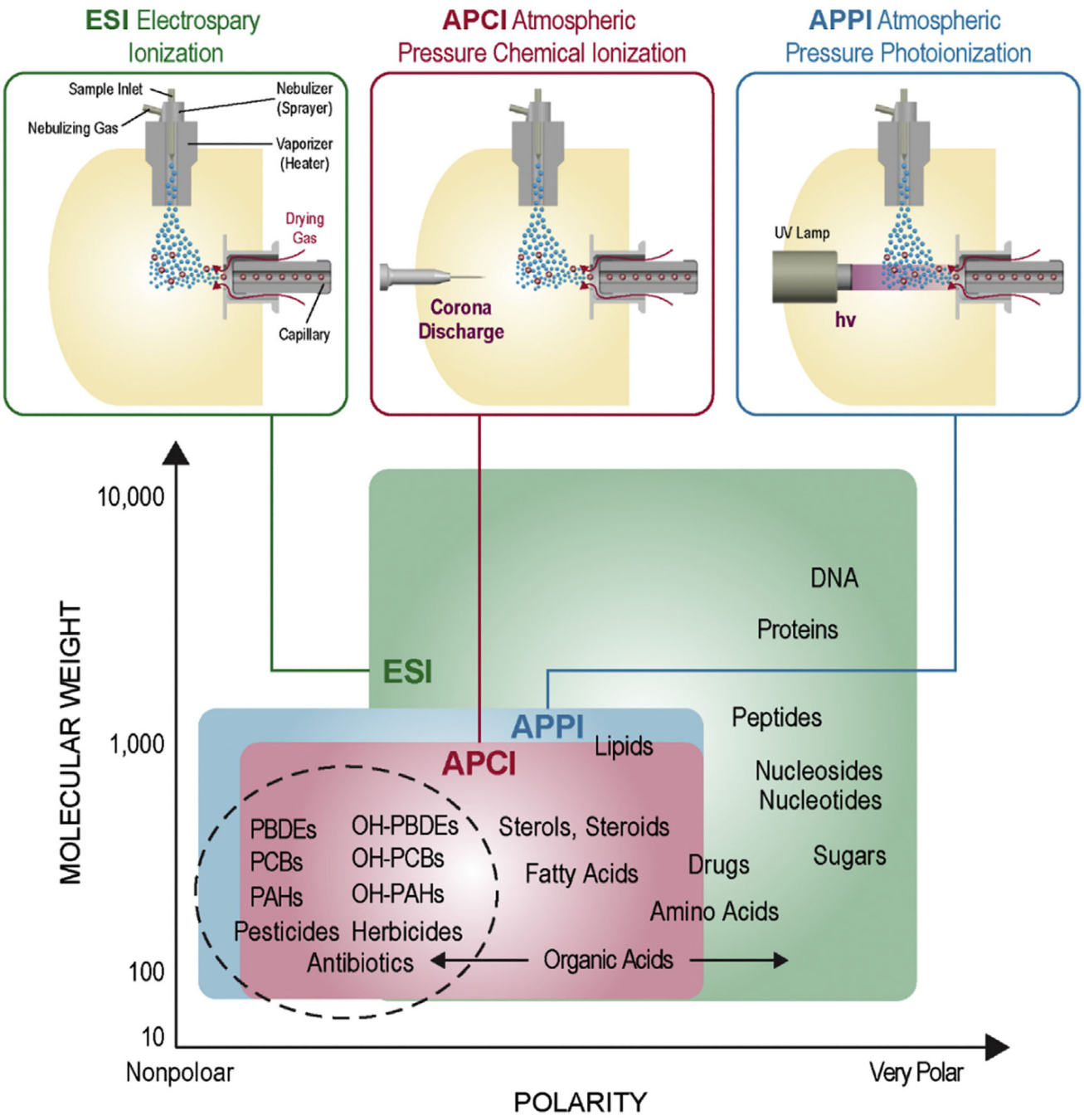

Fig. 2.

Different ionization techniques for polar and nonpolar molecules. Electrospray ionization (ESI) is mainly used for polar compounds, while atmospheric pressure chemical ionization (APCI) and atmospheric pressure photoionization (APPI) are needed for molecules of lower polarity. PAHs: polycyclic aromatic hydrocarbons; OH-PAHs: hydroxylated PAHs; PCBs: polychlorinated biphenyls; OH-PCBs: hydroxylated PCBs; PBDEs: polybrominated biphenyl ethers; OH-PBDEs: hydroxylated PBDEs.

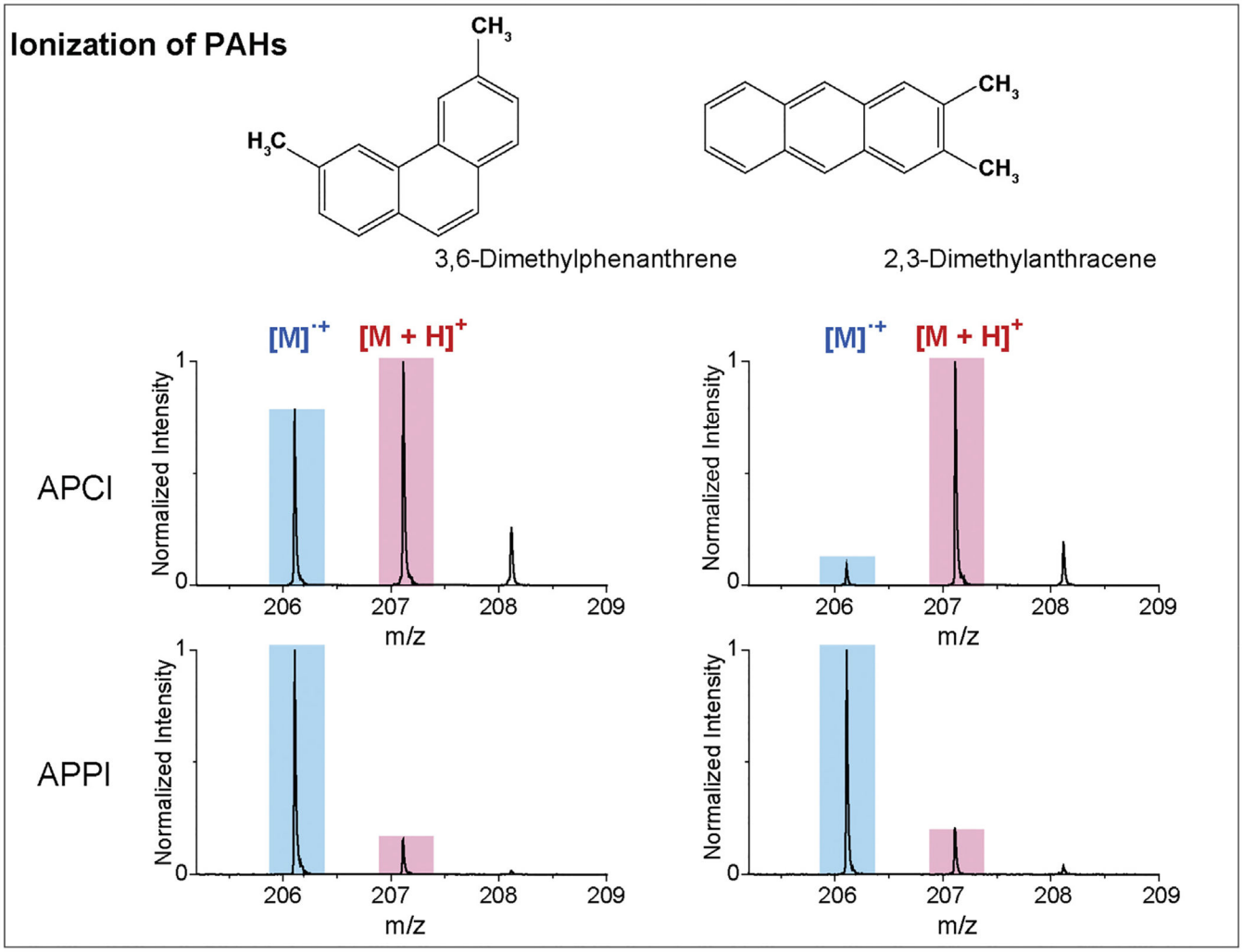

Fig. 3.

PAHs were detected as protonated and/or radical forms using APCI and APPI. Different radical and protonated amounts of 3, 6-Dimethylphenanthrene (36T) and 2, 3-Dimethylanthracene (23D) were observed in the mass spectra due to the difference in the APCI and APPI processes.

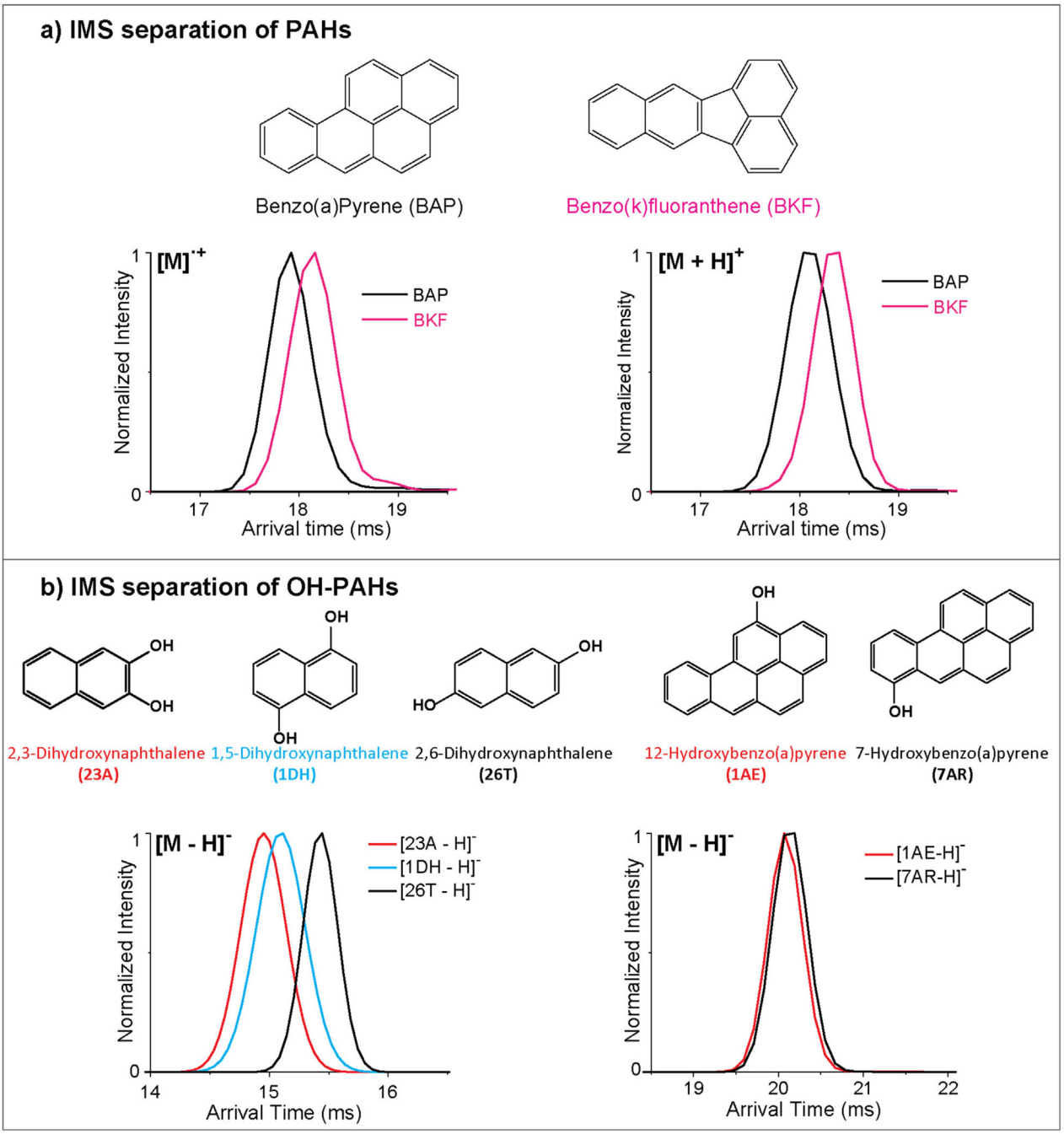

Fig. 4.

IMS separations of a) PAHs and b) OH-PAHs. a) IMS separations of the isomeric PAHs benzo(a)pyrene (BAP) and benzo(k)fluoranthene (BKF) in their radical and protonated forms illustrate BAP is smaller than BKF in both cases. Longer arrival times are observed for the protonated species of both PAHs, illustrating how the proton increases the CCS size.b) IMS separations of isomeric OH-PAHs illustrate a case where IMS is able to distinguish one set of depronated isomers and one case where it cannot. The chemical structure of each molecule is shown.

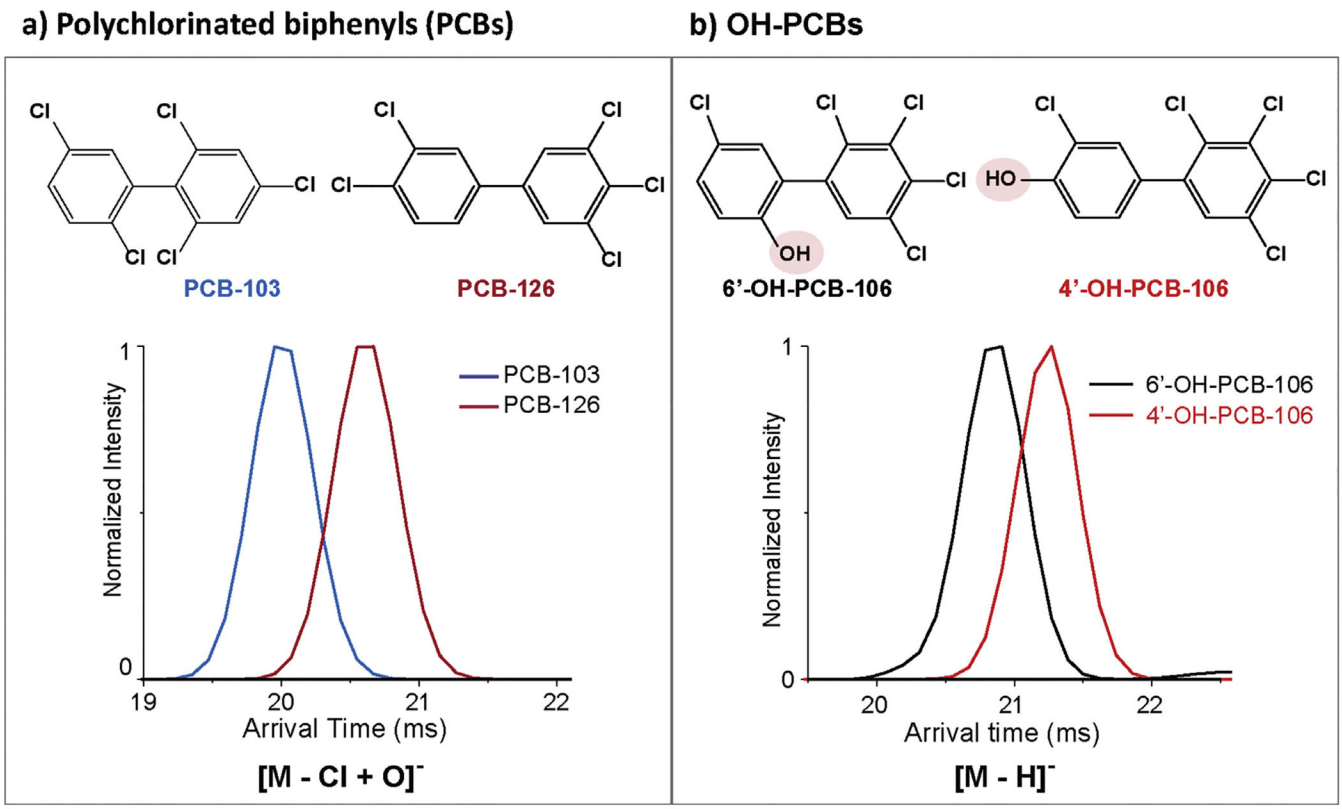

Fig. 5.

IMS separations of a) PCBs and b) OH-PCBs. The position of the functional groups for each molecule illustrates interesting changes in the molecular separations.

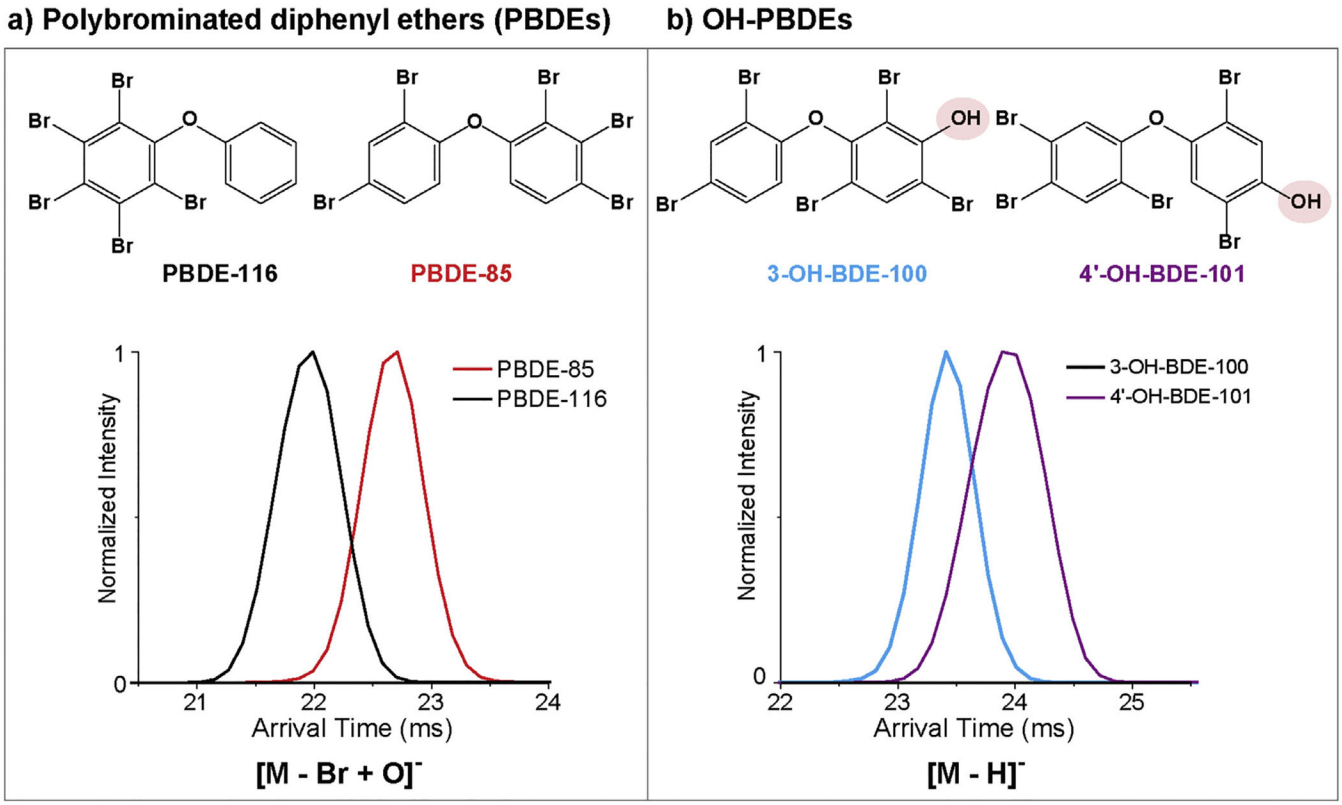

Fig. 6.

IMS separations of a) PBDEs and b) OH-PBDEs again showed that the placement of the function groups influence the total structural size of the molecules.

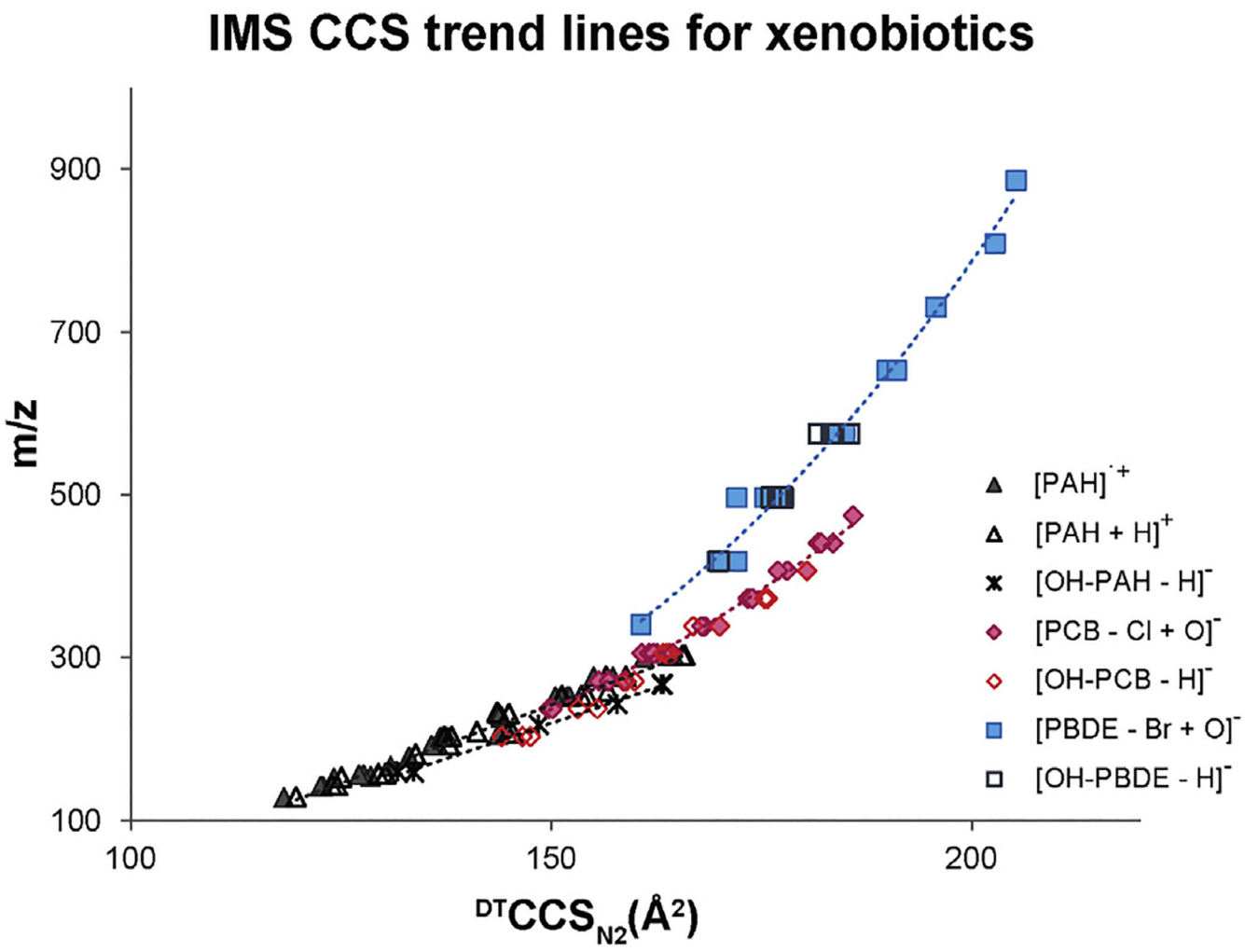

Fig. 7.

CCS versus m/z trend lines for the detected PAHs, PCBs and PBDEs and their metabolites. In most cases, PAHs were found to have the smallest structural sizes relative to the m/z values, while PCBs had the largest.